A Multi-IMU Based Self-contained Pedestrian Navigation Algorithm

Yi-Han Jen [1]*, Chi-Hsin Huang [2], Syun Tsai [1], Kai-Wei Chiang [2]

[1] Department of Geomatics, National Cheng Kung University, Taiwan – (f64084028, p68081500)@gs.ncku.edu.tw
[2] Department of Geomatics, National Cheng Kung University, Taiwan – (windstorm, kwchiang) @geomatics.ncku.edu.tw

KEY WORDS: Inertial Navigation, Inertial Measurement Units, Arbitrary Orientation Estimation, Pedestrian Dead Reckoning, Attitude and Heading Reference System

ABSTRACT:

The demand for navigation and positioning is increasing in various fields nowadays. Although Global Navigation Satellite Systems (GNSS) are currently the most widely used high-accuracy positioning method, their operation rests on signal transmission and reception, which is prone to interference from obstacles such as high-rise buildings, thereby limiting indoor navigation. In addition, in highly dynamic scenarios, the low update rate of the signal cannot track detailed motions. In this case, Inertial Measurement Units (IMUs) play an important role in serving as a complementary component. However, a single high-accuracy IMU is financially prohibitive. On the other hand, the lack of accuracy and stability limits the application of low-cost IMU in navigation. One way to improve the performance of low-cost IMU is to fuse multiple IMUs. This study focuses on the development of pedestrian navigation using multi-sensor integration of low-cost IMUs and magnetometers exploring different integration techniques to compare their performance. The Pedestrian Dead Reckoning (PDR) algorithm is a technique used to estimate the relative motion of pedestrian, which is a commonly used technology for indoor pedestrian navigation. This study use PDR with multi-sensor integration of low-cost IMUs to reduce the position error of pedestrian navigation to within one meter, with the aim of establishing a high-precision, reliable, and low-cost pedestrian navigation algorithm.

1. INTRODUCTION

The emergence of Micro Electro Mechanical Systems (MEMS) level IMUs has increased their potential applications. Although the MEMS-grade IMU is low-accuracy, which accuracy of the gyroscope and accelerometer decreases as the price drops, affecting their performance and stability. However, since the MEMS technology has reduced the volume, power consumption and cost of IMU, combing multiple IMUs in a single Printed Circuit Board (PCB) becomes more available.

The gyroscope is even more critical than the accelerometer in conventional Inertial Navigation System (INS) due to the error from the gyroscope propagated to the overall performance, including orientation, velocity, and position. Among various types of errors, particularly the bias instability of the gyroscope can be very large. Therefore, the bias instability of the gyroscope is the most important error term that dominates the overall performance of the IMU (Alteriis et al., 2021). In general, IMUs can be classified by their performance, from high to low: navigation-grade, tactical-grade, and consumer-grade. The lower the performance, the greater the accumulated error in IMU applications, which can lead to faster drift in position and orientation error. The bias instability of consumer-grade MEMS gyroscopes is typically around 70 degrees per hour (Lee et al., 2016). Such large bias, when integrated under high dynamic motion in any arbitrary orientation of the arm, will result in significant errors in orientation estimation.

Fusing multiple low-accuracy IMUs is one way to improve the performance of a single low-accuracy IMU by leveraging complementary advantages. With the development of MEMS technology and improvements in multi-IMU integration, the balance between the cost and accuracy of IMUs can be achieved. In addition, using multiple low-accuracy MEMS-level IMUs can not only significantly reduce costs but also increase the ability to find errors, increase fault tolerance, and reduce noise. Moreover, high-accuracy IMUs are too large and heavy to be placed in mobile devices, while low-accuracy IMUs can be built into mobile devices and are more suitable for pedestrian navigation applications.

This study focuses on the development of pedestrian navigation using multi-IMU integration of MEMS-grade IMUs. Different integration techniques and fusion methods of multi-IMU will be explored and compared for their performance differences, aiming to obtain the optimal IMU array geometry design and fusion algorithm. The study applies the improved Pedestrian Dead Reckoning (PDR) algorithm to conduct the navigation of pedestrians reaching one-meter positioning accuracy. The goal is to establish high-precision, high-reliability, and low-cost inertial sensors using multi-IMU integration of MEMS-grade IMUs.

2. RELATED WORK

2.1 Inertial Sensor Error

Inertial sensor errors can be classified into two types: systematic errors (also known as deterministicm errors) and stochastic errors (also known as random errors).

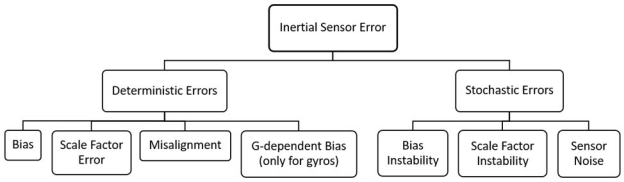

Figure 1. Inertial Sensor Error

* Corresponding author

In the case of an accelerometer, systematic errors can be divided into three types: bias, scale factor errors, and misalignment (Unsal, 2012). When the accelerometer measures an acceleration value without any external acceleration applied, it is called bias. Scale factor error is a proportional relationship between the input and output observation quantities, usually represented in floating-point form with a value range between -1 and 1. Misalignment is an orthogonal error that arises due to imperfect production and installation of sensor components, leading to changes in observation quantities of other axes for any motion on any axis.

For the gyroscope, there are four types of systematic errors: bias, scale factor errors, misalignment, and acceleration-dependent bias (also known as g-dependent bias) (Unsal, 2012). The first three are the same as those of the accelerometer, while acceleration-dependent bias is a deviation in the gyroscope output signal caused by the structural impact of acceleration. The numerical value of the relationship between acceleration and gyroscope measurements is determined by the bias coefficient of acceleration-dependent bias.

Stochastic errors refer to the errors that arise from the random variation over time of bias or scale factor, as well as sensor noise. These errors are respectively known as bias instability, scale factor instability, and sensor noise (Unsal, 2012). And sensor noise can be further divided into three types: angle random walk (ARW), velocity random walk (VRW), and white noise. The most important feature of these errors is that there may be no direct relationship between input and output. Bias instability refers to the changes in bias over time, which can be determined by Allan variance and autocorrelation analysis, and can be modeled using the results of these tests and analyses. Scale factor instability refers to the changes in the scale factor over time, which require long-term dynamic rate tests to determine. Sensor noise can be reduced by filtering

Allan variance, first proposed by David Allan in 1966, is a method of representing the root mean square (RMS) random-drift error as an average time function. Its calculation, interpretation, and understanding are relatively simple. The method was initially used to analyze the instability of the phase and frequency of crystal oscillators or atomic clocks and can be applied to any signal with potential noise. As gyroscopes, accelerometers, and other sensing elements themselves also have oscillator characteristics, this method is now widely used to identify the random errors of various inertial sensors. Calibration via Allan variance analysis typically lasts for several hours.

For MEMS-grade IMUs, systematic errors usually only consider bias and scale factor errors. Because the performance is relatively low compared to other grades, these two errors are significant, while the others are relatively less prominent. Therefore, it is usually ignored for the time being.

2.2 Sensor Array Techniques

In previous examples of fusing multiple low-accuracy IMUs, most methods simply obtained the average specific force and angular rate signals from the array (Bancroft and Lachapelle, 2011). If N IMUs are simply processed by taking the average of the observations, and the observations are independent and the specifications of each IMU are the same, the error propagation of noise can be derived, as shown equations below, and the error can be reduced to 1 over the square root of N, significantly improving performance. This method is the simplest way to achieve a reduction in error, but it does not maximize the reduction in error.

The error propagation of noise equations:

$$\because \bar{X} = \frac{\sum_{i=1}^{N} X_i}{N},\ \sigma_{X_i} = \sigma \tag{1}$$

$$\therefore \sigma_{\bar{X}} = \sqrt{\sum_{i=1}^{N} \frac{\sigma_{X_i}^2}{N^2}} = \sqrt{N \cdot \frac{\sigma^2}{N^2}} = \frac{\sigma}{\sqrt{N}} \tag{2}$$

where X = IMU observations
N = quantity of IMUs
σ = standard deviation

Each systematic error source has four components: a fixed contribution, a temperature-dependent variation, a run-to-run variation, and an in-run variation (Groves, 2007). The array-based IMU composition technology aims to improve the performance of low-cost MEMS-level IMUs. Simply averaging the array information is not enough. In (Martin et al., 2013), it is mentioned that more accurate estimation can be achieved by utilizing the characteristics of the IMUs when setting up multiple IMUs. By placing the sensitive axes of the IMUs in opposite directions, systematic errors between the same type of IMU can be reduced. Among the errors that IMUs may encounter, the specific systematic errors generated by IMUs of the same specification are usually close to or positive or negative values. Therefore, if the sensing axes of the three axes are placed in opposite directions, at least some of the temperature drift can be offset. As for random errors, there is not much difference between the average noise from IMUs on two opposite sensing axes or the average noise from IMUs on two same sensing axes.

2.3 Traditional Pedestrian Dead Reckoning

The Dead Reckoning (DR) algorithm is a technique used to estimate the relative motion of objects. When applied to pedestrians, it is called Pedestrian Dead Reckoning (Fujii and Sakuma, 2018). PDR is a commonly used technology for indoor pedestrian navigation today. This algorithm predicts the position at time k+1 (E_{k+1}, N_{k+1}) based on the known position (E_k, N_k) and azimuth angle φ_k at time t. Most of the time, in order to simplifies the estimation process by assuming that the scenario is walking on a flat surface and reduces the 3D space to a 2D plane to construct an inertial navigation system suitable for general walking situations.

Pedestrian Dead Reckoning equations:

$$\begin{bmatrix} N_{k+1} \\ E_{k+1} \end{bmatrix} = \begin{bmatrix} N_k + SL_k \times cos\varphi_k \\ E_k + SL_k \times sin\varphi_k \end{bmatrix} \tag{3}$$

where k = time
E_k, N_k = the user coordinates at k time
SL_k = step-length at k time
φ_k = azimuth angle at k time

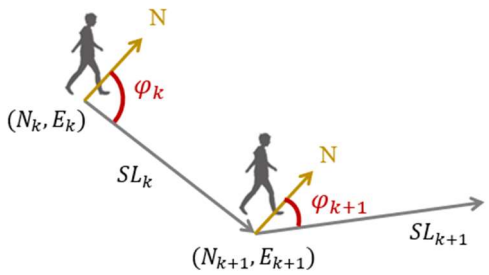

Figure 2. Schematic diagram of the Pedestrian Dead Reckoning principle

Its principle is mainly based on the information obtained from the accelerometer, gyroscope, and magnetometer to calculate the next position, such as the number of steps, stride length, and azimuth, to perform indoor navigation. The accelerometer measures the acceleration and gravitational acceleration of an object in motion and detects the features when people walking to calculate their stride. And then, in combination with an empirical formula, estimate the length of each step. The gyroscope measures the relative rotational angular velocity of an object in motion, and the magnetometer measures the changes in the Earth's magnetic field to determine the object's absolute azimuth. By using both sensors to estimate the azimuth and inputting it into the pedestrian dead reckoning (PDR) formula, the two-dimensional spatial position information can be obtained. The existence of errors in the PDR system is due to the stride length estimation model, which is generally an empirical formula that cannot accurately match the walking habits of each user, and the uncertainty of the model coefficients. Additionally, the errors of the stride length estimation model and the azimuth information accumulate with the number of steps and time, causing the trajectory to gradually drift. Therefore, the PDR system requires external assistance information to limit the accumulation of errors.

In many traditional PDR studies, the value of acceleration magnitude in three-axis direction is used for step detection (Jiménez, 2009). To obtain heading information, it can only be applied when the IMU is perpendicular to the direction of gravity acceleration and cannot support various posture states. Most cases place the IMUs on the ankles or insteps (Jiménez, 2009).

2.4 Attitude Estimation

An Attitude and Heading Reference System (AHRS) includes attitude data calculation and provides information on the attitude and position of an object in space. The attitude information is specified by the prediction of the Roll, Pitch and Yaw angles, known as Euler angles. (Junco, 2017)

If AHRS is used to obtain roll, pitch, and yaw, the obtained roll and pitch can be used to transform the coordinate system to the local level frame, which is commonly used in navigation coordinate systems such as the North-East-Down (NED) frame. By rotating the X-axis and Y-axis of the sensor with gravity acceleration, the Z-axis of the sensor can be aligned with the D-axis of the NED frame, which is called Leveling. The X and Y directions of the sensor can be used for dead reckoning, while the Z direction of the sensor is used for step detection. This method is suitable for devices with non-specific attitudes, such as watches or mobile phones.

3. METHODOLOGY

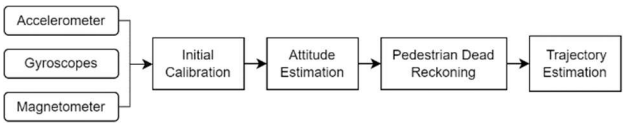

Figure 3. The Multi-IMU Based Self-contained Pedestrian Navigation Algorithm diagram

3.1 Initial Calibration

As mentioned in Section 2.1, for MEMS-grade IMUs, only bias and scale factor errors are usually considered for systematic errors. Therefore, in the experiments conducted in this study, after the sensors start recording data, they are first placed in a static state for a while. The data recorded during this stationary period can be used to estimate the bias and scale factor errors of the gyroscope. These errors of the gyroscope can then be used to perform initial calibration of the experimental data.

The reason why only preliminary calibration is performed on the gyroscope, but not on the accelerometer, is because for PDR navigation applications, unlike in-car navigation or integration system navigation applications, the acceleration value does not play a role in obtaining the moving distance for position calculation through integration. In PDR navigation applications, the acceleration value mainly serves two purposes. First, it is used for step detection, and errors will affect the acceleration values but not the periodical pattern of the steps. Second, it helps with leveling. As the gravity acceleration value is much larger than the error, even if there is an error in the acceleration value, the leveling process is not significantly affected. Therefore, it is currently ignored.

As for the magnetometer, this study used pre-processed 8-shaped movement to obtain the magnetometer errors and perform preliminary calibration on the experimental data for the magnetometer.

3.2 Attitude Estimation

As mentioned in Section 2.4, through AHRS, providing the attitude of the sensor in the North-East-Down (NED) frame, which is then leveled to obtain new attitude information. The horizontal orientation can be used for navigation, while the D direction of the accelerometer is used for step detection. This method can make the navigation estimation more accurate and the gait the pattern more prominent. The process of attitude information calculation in this study is handled by using the Versatile Quaternion-based Filter (VQF). VQF is an extended filter structure by an optional gyroscope bias estimation algorithm and an algorithm for magnetic disturbance detection and rejection. (Laidig et al., 2023)

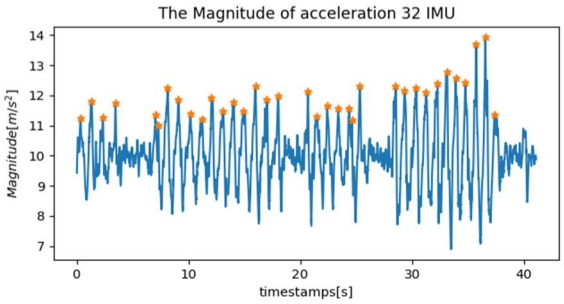

Figure 4. The value of acceleration magnitude in three-axis.

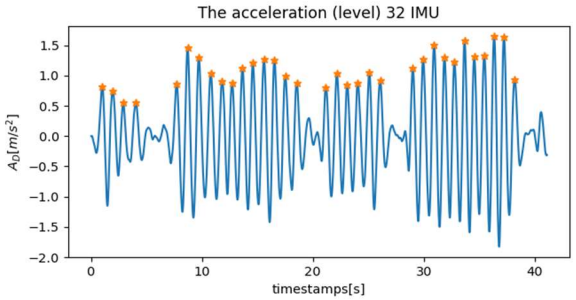

Figure 5. The value of acceleration magnitude in D direction.

Different from the traditional PDR that uses the magnitude of the acceleration vector for step detection (**Figure 4**), this study uses the value of acceleration in the D direction for step detection (**Figure 5**). By using the D direction acceleration value, interference from the horizontal direction is eliminated, and only the vibrations generated when the foot touches the ground during walking or running are shown. This makes the waveform of the vibration more obvious and facilitates accurate identification of the peak position. Therefore, the device is not restricted to a specific posture and can be applied to devices such as smartwatches or mobile phones.

3.3 Pedestrian Dead Reckoning

The Pedestrian Dead Reckoning diagram of this study is shown in **Figure 6**. To simplify the calculation process, it is assumed that the scene is walking on a flat floor, which is simplified to a two-dimensional plane. An empirical model is used to estimate the step length based on personal information such as height, weight, and age. This study uses nine-axis information (including three-axis accelerometers, three-axis gyroscopes, and three-axis magnetometers) to estimate attitude. The D direction of the leveled acceleration value is used for step detection, and the other information is used for heading determination. Finally, the estimated trajectory is plotted.

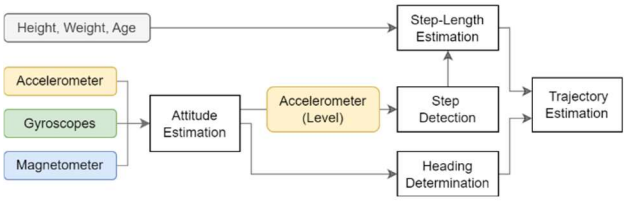

Figure 6. The Pedestrian Dead Reckoning diagram

4. RESULTS AND DISCUSSIONS

The inertial sensors used in this study include Osmium MIMU4844 and MIMU22BL for the combination design of the IMU array. The two sensors were separately tested by hand for indoor and outdoor experiments. In the indoor experiments, the position error is compared between the trajectory position and the control point layout. For outdoor experiments, the position error is calculated using the same starting and ending points.

The MIMU4844 configuration, as shown in **Figure 7**, consists of a total of 32 IMUs. Sixteen IMUs are mounted on the top side with the z-axis pointing downwards (the red text in **Figure 7**), while the other sixteen are mounted on the bottom side with the z-axis pointing upwards (the green text in **Figure 7**).

The MIMU22BL configuration, as shown in **Figure 8** consists of a total of 4 IMUs. Two IMUs are mounted on the top side with the z-axis pointing downwards (the red text in **Figure 8**, while the other two are mounted on the bottom side with the z-axis pointing upwards (the green text in **Figure 8**)

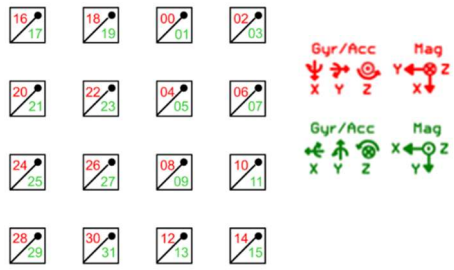

Figure 7. MIMU4844 configuration(red text for IMUs on top side; green text for IMUs on bottom side)

Figure 8. MIMU22BL configuration(red text for IMUs on top side; green text for IMUs on bottom side)

4.1 Allan Variance

As mentioned in Section 2.1, Allan Variance is widely used to identify the random errors of various inertial sensors. We applied Allan Variance to the MIMU4844, and the results are shown in **Figure 9**. The thick green line represents the average of 32 IMUs. As mentioned in Section 2.2, if the observation values of N IMUs are simply averaged and are independent and have the same specification, the error will be significantly reduced.

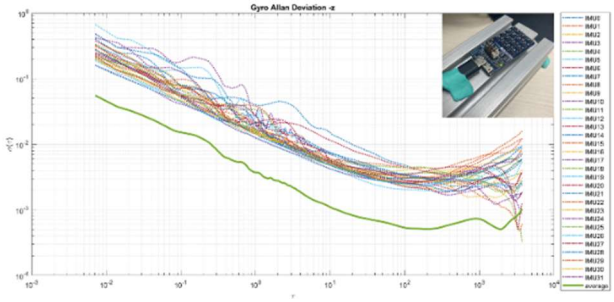

Figure 9. Allan Standard Deviation of MIMU4844

4.2 The Different Quantities of IMUs tested Indoor

As shown in **Figure 10**, it can be seen that the error of a single IMU is larger. The error exceeded one meter at the second control point, and the position error was 2.7941 m. The best result of multi-IMU was achieved with 32 IMUs, and the position error at the fourth control point was 0.3315 m. However, the position errors of the three were not significantly different, all being within one meter, indicating that the result of four IMUs may have already met the current pedestrian navigation requirements in this test scene.

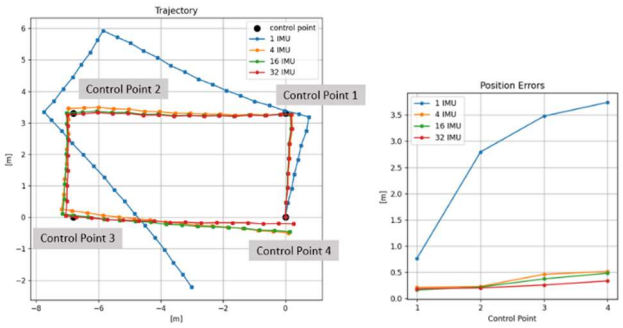

Figure 10. The indoor trajectories and position errors of different quantities of IMUs

	Quantity of IMUs			
Position errors (m)	1 IMU	4 IMUs	16 IMUs	32 IMUs
Control Point 1	0.7612	0.2086	0.1580	0.1808
Control Point 2	2.7941	0.2247	0.2140	0.1975
Control Point 3	3.4789	0.4582	0.3704	0.2529
Control Point 4	3.7424	0.5113	0.4789	0.3315

Table 1. The indoor trajectories and position errors of different quantities of IMUs

4.3 The Front Side and the Back Side of IMUs tested Indoor

As mentioned earlier, the specific systematic errors generated by IMUs are usually almost the same in value and may be positive or negative. Therefore, if the sensing axes are placed in opposite directions, at least some of the temperature drift can be compensated. In **Figure 11**, the error of the IMU array on a single side is larger, with position errors of 0.9654 m and 0.7610 m at the fourth control point. And the array with an equal number of IMUs on both the front and back sides has the smallest error, with a position error of 0.4806 m at the fourth control point.

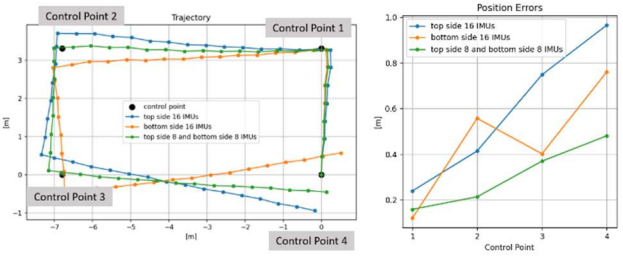

Figure 11. The indoor trajectories and position errors of the front and back sides of IMUs

	The front and back sides of IMUs		
Position errors (m)	top side 16 IMUs	bottom side 16 IMUs	top side 8 and bottom side 8 IMUs
Control Point 1	0.2392	0.1204	0.1586
Control Point 2	0.4143	0.5572	0.2137
Control Point 3	0.7480	0.4016	0.3698
Control Point 4	0.9654	0.7610	0.4806

Table 2. The indoor trajectories and position errors of the front and back sides of IMUs

4.4 The Different Geometric Relationships of IMUs tested Indoor

Different geometrical configurations of IMU arrays were selected to compare position errors, attempting to achieve better precision through geometric constraints. **Figure 7** shows the MIMU4844 configuration diagram. In **Figure 12**, in Figure 3, the symmetric array (the green trajectoty) located far from the center of the IMU array has the smallest error, with a position error of 0.3366m at the fourth control point. The asymmetric array (the red trajectoty) located far from the center of the IMU array has the largest error, with a position error of 0.9146m at the fourth control point.

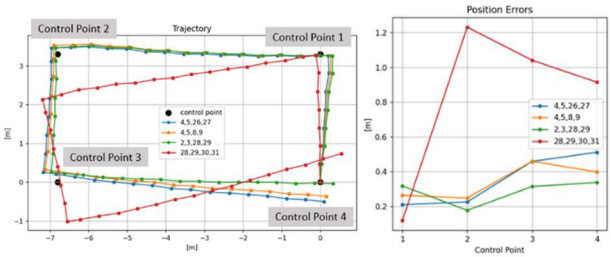

Figure 12. The indoor trajectories and position errors of different geometric relationships of IMUs

	Number of IMUs in MIMU4844			
Position errors (m)	4,5, 26,27	4,5, 8,9	2,3, 28,29	28,29, 30,31
Control Point 1	0.2086	0.2633	0.3172	0.1170
Control Point 2	0.2247	0.2475	0.1764	1.2320
Control Point 3	0.4582	0.4591	0.3139	1.0413
Control Point 4	0.5113	0.3971	0.3366	0.9146

Table 3. The indoor trajectories and position errors of different quantities of IMUs

4.5 The Different Geometric Relationships of IMUs tested Outdoor

Figure 13 shows the trajectory of outdoor preliminary experiments. The test field was the National Cheng Kung University playground, with a distance of 400 meters and starting and ending at the same point. Under high dynamic arbitrary postures of arm swinging, the algorithms used in this study were able to demonstrate high-precision trajectory results. As for how to calculate high dynamic posture changes, we have another algorithm to solve it, which is not the focus of this study.

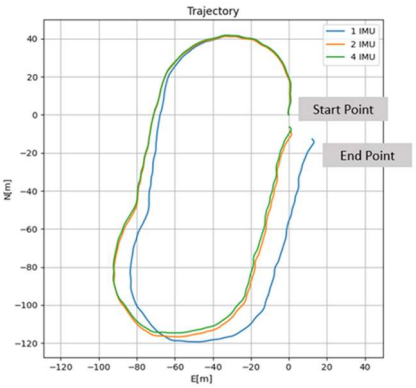

Figure 13. The outdoor trajectories of different quantities of IMUs

5. CONCLUSIONS

The results from Section 4.2 to 4.5 demonstrate that the results of multiple IMUs are better match actual walking paths than a single IMU. And the consequent regardless of indoor or outdoor settings or different brands and specifications.When an array of 4 IMUs is reached, the positioning error of pedestrian navigation is reduced to within one meter, meeting current demands for pedestrian navigation. The benefit of increasing the number of IMUs to 16 or 32 is diminishing. In addition, the results of the geometric relationships of the IMU array are consistent with (Martin et al., 2013) paper. Systematic errors generated by sensors of the same specifications are usually nearly the same or either positive or negative values. Therefore, if the sensing axes are placed in the opposite directions, at least some temperature deviation drift can be eliminated.

Through multiple testing iterations, it was found that excessive magnetic field interference in the indoor experimental field led to unexpected results. Therefore, the magnetic compass was not used in indoor experiments in this study. Magnetic field interference may also occur in outdoor fields, so in the future, an automatic mechanism for detecting magnetic interference could be conducted. By exclude those interfered magnetic measurement, the distorted results of IMU arrays can be reduced.

The results of this study show that multiple IMUs can construct a vertual, low-cost, high-accuracy, and high-reliability inertial sensor. It is more suitable for navigation on watches or mobile devices and can be used indoors and outdoors. Multiple IMUs have considerable potential.

REFERENCES

Alteriis, G.D., Accardo, D., Conte, C., & Moriello, R.S., 2021. “Performance Enhancement of Consumer-Grade MEMS Sensors through Geometrical Redundancy.” Sensors (Basel, Switzerland), 21.

Lee, J., Jang, S., Choi, J.G., & Lee, T.G., 2016. “North-Finding System Using Multi-Position Method With a Two-Axis Rotary Table for a Mortar.” IEEE Sensors Journal, 16, 6161-6166.

Bancroft, J., & Lachapelle, G., 2011. “Data Fusion Algorithms for Multiple Inertial Measurement Units. Sensors” (Basel, Switzerland), 11, 6771 - 6798.

Unsal, D., & Demirbas, K., 2012. “Estimation of deterministic and stochastic IMU error parameters.” Proceedings of the 2012 IEEE/ION Position, Location and Navigation Symposium, 862-868.

Groves, P.D., 2007: *Principles of GNSS, Inertial, and Multi-Sensor Integrated Navigation Systems.*

Martin, H., Groves, P.D., Newman, M., & Faragher, R., 2013. “A New Approach to Better Low-Cost MEMS IMU Performance Using Sensor Arrays.”

Fujii, M., & Sakuma, Y., 2018. “Suppression of performance degradation in traveling direction estimation by using IMU and PCA for PDR.” Int. J. Netw. Comput., 8, 328-340.

Jiménez, A.R., Seco, F., Prieto, C., & Guevara, J. 2009. “A comparison of Pedestrian Dead-Reckoning algorithms using a low-cost MEMS IMU” 2009 IEEE International Symposium on Intelligent Signal Processing, 37-42.

Junco, A.H., & Fernández, J.R. 2017. “Design and Implementation of an Attitude and Heading Reference System (AHRS) using Direction Cosine Matrix.”

Laidig, Daniel, and Thomas Seel. 2023. “VQF: Highly Accurate IMU Orientation Estimation with Bias Estimation and Magnetic Disturbance Rejection.” Information Fusion 91: 187–204.